

ChemComm

Chemical Communications

Accepted Manuscript

This article can be cited before page numbers have been issued, to do this please use: R. He, Y. Zhang, S. Madhu, Q. Gao, Q. Lian, S. S. Raghavan and J. Geng, *Chem. Commun.*, 2020, DOI: 10.1039/D0CC06313D.



This is an Accepted Manuscript, which has been through the Royal Society of Chemistry peer review process and has been accepted for publication.

Accepted Manuscripts are published online shortly after acceptance, before technical editing, formatting and proof reading. Using this free service, authors can make their results available to the community, in citable form, before we publish the edited article. We will replace this Accepted Manuscript with the edited and formatted Advance Article as soon as it is available.

You can find more information about Accepted Manuscripts in the [Information for Authors](#).

Please note that technical editing may introduce minor changes to the text and/or graphics, which may alter content. The journal's standard [Terms & Conditions](#) and the [Ethical guidelines](#) still apply. In no event shall the Royal Society of Chemistry be held responsible for any errors or omissions in this Accepted Manuscript or any consequences arising from the use of any information it contains.

COMMUNICATION

BODIPY Based Realtime, Reversible and Targeted Fluorescent Probes for Biothiols Imaging in Living CellsRongkun He,^{a, b} Yichuan Zhang,^a Suresh Madhu,^a Quan Gao,^a Qianjin Lian,^a Sriram Srinivasa Raghavan^c and Jin Geng^{a, *}Received 00th January 20xx,
Accepted 00th January 20xx

DOI: 10.1039/x0xx00000x

Real-time live cell imaging and quantification of biothiols dynamics are important for understanding the pathophysiological process. However, it is still challenging in the design and synthesis of rational probes that have reversible and real-time capabilities. In this work, we have prepared Boron-dipyrromethene (BODIPY) based fluorescent molecules as ratiometric probes that allow the real-time biothiols dynamics in living cells. The Michael reaction between α -formyl-BODIPY (BOD-JQ) and GSH exhibited a reversible fluorogenic mechanism with fluorescent emission shifting from 592 nm to 544 nm with $t_{1/2} = 16$ ms. In particular, we showed that the probes with targeting agents are capable of detecting biothiols in mitochondria and endoplasmic reticulum (ER) with high temporal resolution.

Biothiols play crucial roles in maintaining biological redox homeostasis in biological systems.^{1,2,3,4,5,6} Alterations of the cellular thiols levels have been found to relate a number of diseases, such as leucocyte loss,^{7,8,9,10} cancer,^{11,12,13} AIDS,¹² Alzheimer's disease,^{14, 15} psoriasis⁵ and liver damage.^{16, 17, 18, 19, 20, 21} Such fundamental biological roles explain the considerable contemporary effort devoted to the development of efficient methods for the detection and quantification of biothiols.



Scheme 1. Reversible reaction of BOD-JQ with thiols.

^a Institute of Biomedicine and Biotechnology, Shenzhen Institutes of Advanced Technology, Chinese Academy of Sciences, Shenzhen, China.^b College of Chemistry and Chemical Engineering, Xiamen University, Xiamen, China.^c Molecular Biophysics Unit, Indian Institute of Science, Bangalore, India.

† Electronic Supplementary Information (ESI) available. See DOI: 10.1039/x0xx00000x

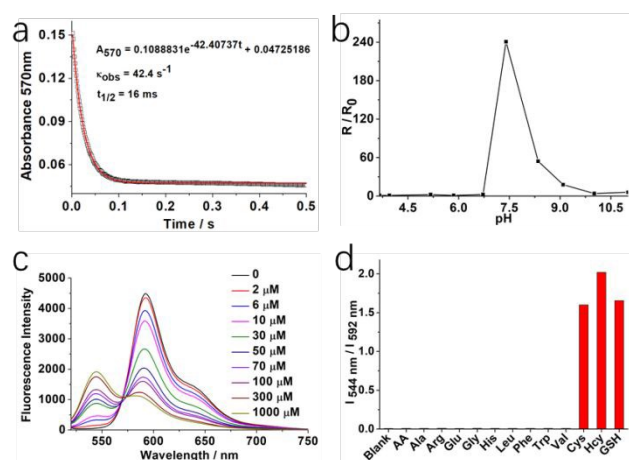


Figure 1. (a) Time course of the response of BOD-JQ to GSH. Kinetic studies were performed using a stopped-flow spectrophotometer at 25 °C under pseudo-first-order conditions (5 μ M BOD-JQ and 1 mM GSH). (b) Effect of pH on the fluorescence responses of BOD-JQ (5 μ M) to GSH (500 μ M), R_0 is the ratio of $I_{544\text{ nm}} / I_{592\text{ nm}}$ of BOD-JQ, R is the ratio of $I_{544\text{ nm}} / I_{592\text{ nm}}$ of BOD-JQ in the presence of GSH. (c) Fluorescence emission spectra ($\lambda_{\text{exc}} = 510$ nm) of BOD-JQ (5 μ M) upon the addition of GSH. (d) Fluorescence intensity ratio ($I_{544\text{ nm}} / I_{592\text{ nm}}$) of BOD-JQ (5 μ M) toward substance to be detected (500 μ M) Reaction solvent: DMSO : H₂O : PBS = 14 : 5 : 1 (v : v : v), PBS: 0.2 M potassium phosphate buffer, pH 7.4.

Many efforts have been made to develop fluorescent probes for detecting biothiols. However, many of them showed slow response and thus cannot be used for real-time detection. To date, only a limited number of real-time fluorescent probes for biothiol detections have been reported, of which the equilibrium can be reached within one minute.^{17, 22} However drawbacks such as complicated synthesis route²¹ and narrow emission shift (≤ 39 nm) resulted in high background interferences²² and the response mechanism based on turn-on fluorescence response¹⁷ (see Supplementary Table 1).

BODIPY and its diversities is one of the most exploited fluorophores and has played a pivotal role in fluorescent probe developments.¹⁶ However, there has not been any BODIPY based biothiol probes reported for biothiol detections with reversible and fast reaction kinetics^{23, 24} (see Supplementary

Table 1). Therefore, it is of great significance to develop a BODIPY-based probe to overcome the drawbacks discussed above allowing real-time detection of biothiols in living cells.

Herein, we introduce a robust BODIPY-based molecular fluorescent probe that enabled a real-time sensing, ratiometric and continuous monitoring of biothiols in living cells. The probe was designed to rapidly and reversibly react with biothiols (Scheme 1). We observed that these probes can react with biothiols, including GSH, Cys, Hcy, resulting in a shifted emission for about 50 nm from 592 nm to 544 nm. The reversibility of the reaction was successfully demonstrated using the GSH and N-ethylmaleimide (NEM) in aqueous solutions and living cells (Supplementary Movie S1 and S2). In addition, BOD-JQ was reacted with Cys or Hcy and then NEM to demonstrate their reversibility with biothiols. Supplementary Movie 3 and 4 showed strong evidence that BOD-JQ react with Cys and Hcy in a reversible manner, too. In particular, we have shown that the probes with targeting moieties are capable of measuring biothiols dynamics in mitochondria and endoplasmic reticulum (ER) with a high temporal resolution.

To detect biothiols in biological systems, we have designed and synthesized an α -formyl-BODIPY dye with a carbon-carbon double bond for Michael addition with biothiols (BOD-JQ, Figure 1a). To accelerate the reaction rate of Michael addition, electron-withdrawing groups were introduced to the α -position as reported,²⁶ *i.e.* probe **1** (with an ester group), **6** (with a cyano group) and **7** (with an aldehyde group) in Supplementary Table 1. It is worth noting that some electron withdrawing groups, such as nitro groups, reduced the reaction rates.²⁷ In this work, we have chosen aldehydes to modify the BODIPY core. We found that the obtained probe, BOD-JQ, reacted with GSH within 0.2 s in an aqueous solution (PBS/DMSO, 3/7). Figure 1a showed the time-dependent response of BOD-JQ to GSH in a pseudo-first-order reaction manner (5 μ M BOD-JQ with 1 mM GSH). The observed rate constant (k_{obs}) at pH 7.4 and 25 °C was found 42.4 s⁻¹ ($t_{1/2}$ = 16 ms), indicating BOD-JQ can rapidly react with GSH under such experimental conditions.

We then investigated the influences of pH on the reaction of BOD-JQ with GSH. The most significant fluorescence intensity change upon reacting with GSH was observed at pH 7.4, as shown in Figure 1b (R/R_0 = 240.7, where R_0 and R are $I_{544\text{ nm}}$ / $I_{592\text{ nm}}$ in the absence and presence of GSH, respectively). BOD-JQ showed ratiometric fluorescence responses with a wide dynamic range and exhibited a maximum fluorescence intensity at 592 nm and 544 nm before and after the reaction with GSH, respectively (Figure 1c and Supplementary Figure S27). The fluorescence intensity ratio ($I_{544\text{ nm}} / I_{592\text{ nm}}$) was found to be linearly related to the GSH concentration in the range of 4 μ M - 70 μ M with R^2 = 0.997 (Supplementary Figure S47).

Selectivity is an important parameter in evaluating the performance of a probe. Commonly existed biomolecules in living systems, including amino acids and ascorbic acid, were used to evaluate the reaction selectivity of BOD-JQ with biothiols. We observed that the addition of biothiols gave a notable change in fluorescence intensities, while all other reagents gave neglectable changes upon biothiol additions (Figure 1d). The competition experiments were carried out by

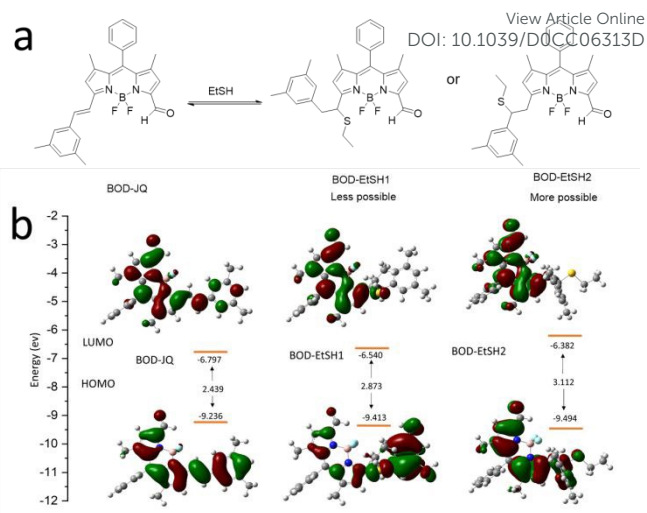


Figure 2. Electron density distributions in the HOMO and LUMO. (a) Scheme of reversible reaction of BOD-JQ with EtSH and the possible product. (b) Electron density distributions in the HOMO and LUMO of BOD-JQ, BOD-EtSH1 and BOD-EtSH2. Color code: C (gray), H (white), O (red), N (blue), F (light green), B (pink), S (yellow).

adding GSH (100 equiv.) to a solution of BOD-JQ (5 μ M) in the presence of amino acids or ascorbic acid (100 equiv.). The results revealed that the reaction of BOD-JQ with biothiols was not significantly interfered (Supplementary Figure S50).

The reversibility of the reaction between BOD-JQ and GSH was demonstrated by the addition of N-ethylmaleimide (NEM) (1 equiv. to GSH, 1 mM) to the reaction mixture. The reaction was monitored by measuring the absorbance at 570 nm of the reaction solution after the addition of GSH and NEM. The absorbance of the BOD-JQ at 570 nm decreased immediately after the addition of GSH, and the subsequent addition of NEM resulted in a rapid and complete recovery of the intensity, even after three cycles, confirming the reversibility of the reaction (Supplementary Figure S51). The colour changes of the solution can be directly visualized by naked eyes as shown in Supplementary Figure S52 and Supplementary Movie 1).

Due to the reversibility of the Michael addition between BOD-JQ and GSH, the dissociation of GSH from BOD-JQ can be evaluated without a scavenger. As "Dilution" favors the dissociation and reforming of BOD-JQ. Thus, we have further confirmed the reversibility of the reaction, because the absorbance of solution C (570 nm) was more than half of B, and has the same intensity as that of A (Supplementary Figure S53).

Molecular descriptors of the BODIPY dye were calculated using Density functional theory (DFT) calculations. Ethanethiol (EtSH) was used to react with BOD-JQ giving two possible products BOD-EtSH1 and BOD-EtSH2 as shown in Figure 2a. The energy difference between highest occupied molecular orbital (HOMO) and lowest unoccupied molecular orbital (LUMO) has been used as an easiest indicator for the kinetic stability.²¹ A large HOMO-LUMO energy gap implied the high kinetic stability or low chemical reactivity of the molecules, because the favorability of the addition or extraction of electrons

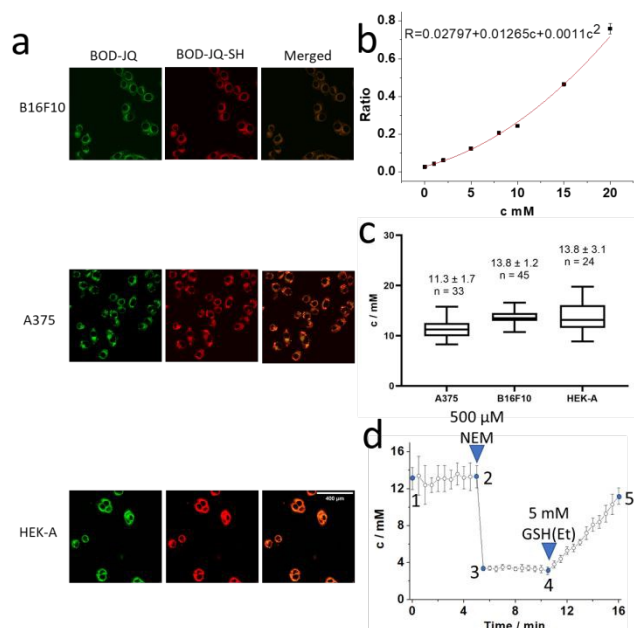


Figure 3. Quantification of biothiols in several cell lines. (a) Confocal fluorescence images of B16F10, A375 and HEK-A Cells incubated with BOD-JQ (2 μM) for 30 min: green channel at 500 – 550 nm (BOD-JQ-SH), λ_{ex} = 488 nm, red channel at 570 – 620 nm (BOD-JQ), λ_{ex} = 561 nm. (b) Calibration curve of GSH concentration against the intensity ratio of green and red channels. The plots were fitted with a quadratic equation, and the calculated fitting equation is given in the graph as $R = 0.02797 + 0.01265c + 0.0011c^2$, where R represents for intensity ratio of green and red channels, and c represents for GSH concentration. (c) Box plots of biothiols concentration in each cell line calculated via the equation showing in (b). Values (mM) above each box plot represent mean \pm s.d. (n is the number of cells). Scale bar = 400 μm. (d) Calculated real time biothiols concentration in living B16F10 cells. Error bars represent standard deviation (n = 19 cells).

from a low-lying HOMO indicated by this energy gap. The simulation studies gave the energy gap of BOD-EtSH2 as 3.112 eV and BOD-EtSH1 as 2.873 eV, suggesting the formation of BOD-EtSH2 was more favorable and stable than BOD-EtSH1. This result is in well agreement with previous studies.^{12, 27, 28}

As discussed, the probe exhibited high sensitivity, selectivity and ratiometric fluorescent responses to biothiols. We therefore continued to investigate the reaction of the probes with biothiols in living cells. We incubated BOD-JQ with several cell lines, including B16F10 (mouse melanoma cells), HEK-A (human epidermal keratinocyte) and A375 cells (malignant melanoma cells). 2 μM was chosen as the concentration of BOD-JQ for further studies because of the compatibility of the probe (> 85% viability at this concentration) (Supplementary Figure S54 – S62).

All the cell lines (B16F10, HEK-A and HEK-A) were incubated with BOD-JQ (2 μM) for 30 min. We observed that BOD-JQ-SH was shown in green and BOD-JQ was shown in red (Figure 3a), confirming sufficient cellular permeability of the probe and the Michael addition reactions happened in cells as expected. The fluorescent signal ratios varied between cell lines, implying the differences in biothiols level in these cells. The fluorescence intensity ratio between BOD-JQ-SH and BOD-JQ

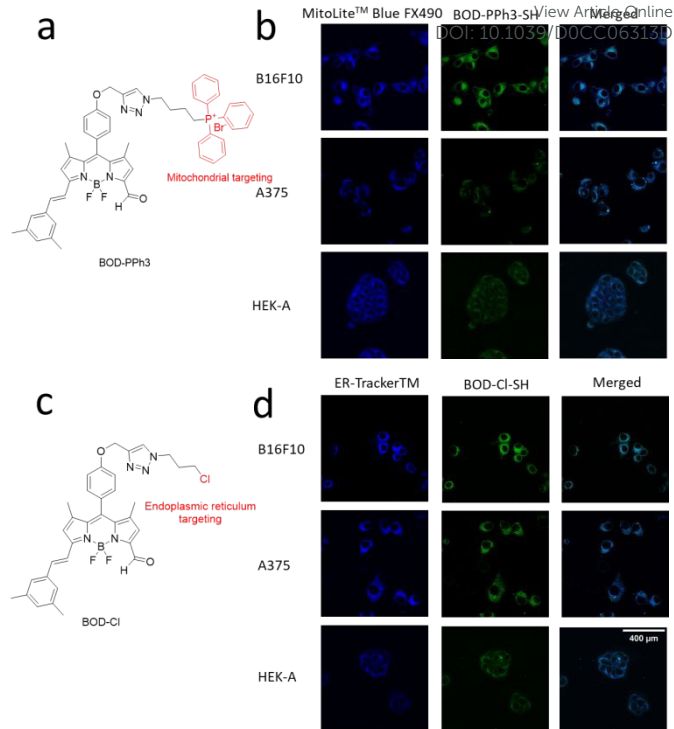


Figure 4. Targeting fluorescent probes. (a) BOD-PPh3 with targeting group for mitochondrial. (b) Confocal fluorescence images of B16F10, A375 and HEK-A cells incubated with BOD-PPh3 (2 μM) for 30 min. followed by containing with MBF for 5 min, from left to right: blue 430 – 470 nm, λ_{ex} = 405 nm (MBF); green 500 – 550 nm, λ_{ex} = 488 nm (BOD-PPh3-SH); merged images of blue and green channels (c) BOD-Cl with targeting group for ER. (d) Confocal fluorescence images of B16F10, A375 and HEK-A Cells incubated with probe BOD-Cl (2 μM) for 30 min followed by containing with ERT for 5 min, from left to right: blue channel at 430 – 470 nm, λ_{ex} = 405 nm (ERT); green channel at 500 – 550 nm, λ_{ex} = 488 nm (BOD-Cl-SH); merged images of blue and green channels.

against biothiols concentrations were fitted well in a quadratic equation (Figure 3b). Therefore, we were able to calculate the intracellular biothiols concentrations based on this equation *i.e.*, 11.3 ± 1.7 mM for A375 cells, 13.8 ± 1.2 mM for B16F10 cells, and 13.8 ± 3.1 mM for HEK-A (Figure 3c). The biothiols concentrations in these cells determined by the BOD-JQ probes were in agreement with previously reported values,^{15, 28} indicating the potential applications of our probes and methodologies in quantifying intracellular biothiol concentrations.

The significant biological roles of biothiols has explained the considerable contemporary effort devoted to the development of efficient methods for the detection and quantification of biothiols in different organelles. In this work, we have prepared two organelle-targeting probes, BOD-PPh3 and BOD-Cl, functionalized with mitochondria targeting group and ER targeting group as shown in Figure 4a and 4c. We incubated B16F10 cells with the probes under the same conditions as discussed above. Colocalization experiments were carried out using two commonly employed mitochondrial tracker and ER tracker. We observed that the fluorescence of Mito-tracker was well colocalized with that of reacted BOD-PPh3 in cells, with Pearson's correlation coefficients (Rr) determined as 0.85 for B16F10 cells, 0.88 for A375 cells, and 0.82 for HEK-A (Figure

4b). The similar level of colocalization was observed for ER targeting probe, BOD-Cl (Figure 4d), where we determined the Pearson's correlation coefficients were 0.86 for B16F10 cells, 0.86 for A375 cells, and 0.89 for HEK-A. In the contrast, when using probe, BOD-JQ, without any targeting agents, the Pearson's correlation coefficients were found as poor as 0.21 for both mitochondria and ER in B16F10, a375 and HEK-A cells (supplementary Figure S63).

We have successively demonstrated that BOD-JQ can reflect the changes of the intracellular biothiol concentrations. The cellular biothiol level was manipulated by the addition of NEM and the cell-permeable glutathione monoethyl ester (a GSH precursor). Initially, we incubated BOD-JQ (2 μ M) with B16F10 cells for 30 min. After the addition of NEM (500 μ M), the fluorescence intensity of BOD-JQ-SH decreased rapidly and reached a plateau within 30s. This was due to the disassociation of BOD-JQ and the re-formation of BOD-JQ. We observed that the fluorescence intensity was unchanged without further treatments. After 5 min, GSH monoethyl ester (5 mM) was added and the fluorescence intensity was gradually restored, indicating the detection of intracellular biothiols changes in real time by BOD-JQ (Supplementary Figure S64 and Figure 3d).

In summary, we have rationally designed and synthesized a highly sensitive BODIPY-based fluorescence probe which exhibited tremendous fast reaction kinetics with thiols, thus it enabled the real-time monitoring of biothiols concentrations in living cells. We demonstrated the probe for quantifying intracellular GSH concentration by measuring GSH levels in various cell lines and by successfully monitoring the GSH dynamics in living cells. The results presented here support our view that these probes are valuable tools for the investigation of how thiols dynamics are regulated in a physiological context, due to their capability for real-time quantification of biothiols with high temporal resolution. We envision that these new probes will enable opportunities to study biothiols dynamics and transportation and expand our understanding of the physiological and pathological roles of biothiols in living cells.

This work was completed with support by National Natural Science Foundation of China (22071263), Hundred-Talent Program (Chinese Academy of Sciences) and Guangdong Natural Science Foundation (2020A1515010994).

Conflicts of interest

There are no conflicts to declare

Notes and references

1. J. Yin, Y. Kwon, D. Kim, D. Lee, G. Kim, Y. Hu, J.-H. Ryu and J. Yoon, *J. Am. Chem. Soc.*, 2014, **136**, 5351-5358.
2. B. Helbling, J. Von Overbeck and B. H. Lauterburg, *Eur. J. Clin. Invest.*, 1996, **26**, 38-44.
3. X.-F. Yang, Q. Huang, Y. Zhong, Z. Li, H. Li, M. Lowry, J. O. Escobedo and R. M. Strongin, *Chem. Sci.*, 2014, **5**, 2177-2183.
4. Y.-F. Kang, L.-Y. Niu and Q.-Z. Yang, *Chin. Chem. Lett.*, 2019, **30**, 1791-1798.
5. Y. Yue, F. Huo, F. Cheng, X. Zhu, T. Mafireyi, R. M. Strongin and C. Yin, *Chem. Soc. Rev.*, 2019, **48**, 4155-4177.

6. Y. Yue, C. Yin, F. Huo, J. Chao, Y. Zhang, *Sens. Actuators B Chem.* 2016, **223**, 496-500. DOI: 10.1039/D0CC06313D
7. D. M. Townsend, K. D. Tew and H. Tapiero, *Biomed. Pharmacother.*, 2003, **57**, 145-155.
8. J. M. Estrela, A. Ortega and E. Obrador, *Crit. Rev. Clin. Lab. Sci.*, 2006, **43**, 143-181.
9. X. Yang, Y. Guo and R. M. Strongin, *Angew. Chem., Int. Ed.*, 2011, **50**, 10690-10693.
10. S. Seshadri, A. Beiser, J. Selhub, P. F. Jacques, I. H. Rosenberg, R. B. D'Agostino, P. W. F. Wilson and P. A. Wolf, *N. Engl. J. Med.*, 2002, **346**, 476-483.
11. L.-Y. Niu, Y.-S. Guan, Y.-Z. Chen, L.-Z. Wu, C.-H. Tung and Q.-Z. Yang, *J. Am. Chem. Soc.*, 2012, **134**, 18928-18931.
12. L. Yi, H. Li, L. Sun, L. Liu, C. Zhang and Z. Xi, *Angew. Chem., Int. Ed.*, 2009, **48**, 4034-4037.
13. H. Jiang and H. Ju, *Anal. Chem.*, 2007, **79**, 6690-6696.
14. K. Amarnath, V. Amarnath, K. Amarnath, H. L. Valentine and W. M. Valentine, *Talanta*, 2003, **60**, 1229-1238.
15. F. Wang, L. Zhou, C. Zhao, R. Wang, Q. Fei, S. Luo, Z. Guo, H. Tian and W.-H. Zhu, *Chem. Sci.*, 2015, **6**, 2584-2589.
16. T. Matsumoto, Y. Urano, T. Shoda, H. Kojima and T. Nagano, *Org. Lett.*, 2007, **9**, 3375-3377.
17. B. K. McMahon and T. Gunnlaugsson, *J. Am. Chem. Soc.*, 2012, **134**, 10725-10728.
18. X. Xie, M. Li, F. Tang, Y. Li, L. Zhang, X. Jiao, X. Wang and B. Tang, *Anal. Chem.*, 2017, **89**, 3015-3020.
19. Meister, A.; Anderson, M. E. *Annu. Rev. Biochem.* 1983, **52**, 711-760
20. Z. Lu, Y. Lu, C. Fan, X. Sun, M. Zhang and Y. Lu, *J. Mater. Chem. B*, 2018, **6**, 8221-8227.
21. Z. Cai, X. Liu, X. Wang, Z. Chen, Z. Song, Y. Xu, H. Tao, Y. Li, R. Chen, L. Guo and F. Fu, *Anal. Chim. Acta*, 2019, **1091**, 127-134.
22. K. Umezawa, M. Yoshida, M. Kamiya, T. Yamasoba and Y. Urano, *Nat. Chem.*, 2017, **9**, 279-286.
23. J. Zhang, N. Wang, X. Ji, Y. Tao, J. Wang and W. Zhao, *Chem. - Eur. J.*, 2020, **26**, 4172-4192.
24. X. Jiang, J. Chen, A. Bajić, C. Zhang, X. Song, S. L. Carroll, Z.-L. Cai, M. Tang, M. Xue, N. Cheng, C. P. Schaaf, F. Li, K. R. MacKenzie, A. C. M. Ferreón, F. Xia, M. C. Wang, M. Maletić-Savatić and J. Wang, *Nat. Commun.*, 2017, **8**, 16087.
25. E. H. Krenske, R. C. Petter and K. N. Houk, *J. Org. Chem.*, 2016, **81**, 11726-11733.
26. H. Hino, M. Kamiya, K. Kitano, K. Mizuno, S. Tanaka, N. Nishiyama, K. Kataoka, Y. Urano and J. Nakajima, *Transl. Oncol.*, 2016, **9**, 203-210.
27. Y. Urano, M. Sakabe, N. Kosaka, M. Ogawa, M. Mitsunaga, D. Asanuma, M. Kamiya, M. R. Young, T. Nagano, P. L. Choyke and H. Kobayashi, *Sci. Transl. Med.*, 2011, **3**, 110-119.
28. S.-Y. Lim, K.-H. Hong, D. I. Kim, H. Kwon and H.-J. Kim, *J. Am. Chem. Soc.*, 2014, **136**, 7018-7025.

